RED-ACT Report

Real-time Earthquake Damage Assessment using City-scale Time-history analysis

June 18, M6.8 Japan Yamagata-ken Oki Earthquake

Research group of Xinzheng Lu at Tsinghua University (luxz@tsinghua.edu.cn)

First reported at 21:45, June 18, 2019 (Beijing Time, UTC +8)

Acknowledgments and Disclaimer

The authors are grateful for the data provided by K-NET and KiK-net. This analysis is for research only. The actual damage resulting from the earthquake should be determined according to the site investigation.

Scientific background of this report can be found at:

http://www.luxinzheng.net/software/Real-Time_Report.pdf

1. Introduction to the earthquake event

At 22:22 JST 18 Jun 2019 (Local Time, UTC +9), an M 6.8 (JMA) earthquake occurred in Japan Yamagata-ken Oki. The epicenter was located at 139.5 38.6, with a depth of 10.0 km.

2. Recorded ground motions

25 ground motions near to epicenter of this earthquake were analyzed. The names and locations of the stations can be found Table 1. The maximal recorded peak ground acceleration (PGA) is 331 cm/s/s. The corresponding response spectra in comparison with the design spectra specified in the Chinese Code for Seismic Design of Buildings are shown in Figure 1.

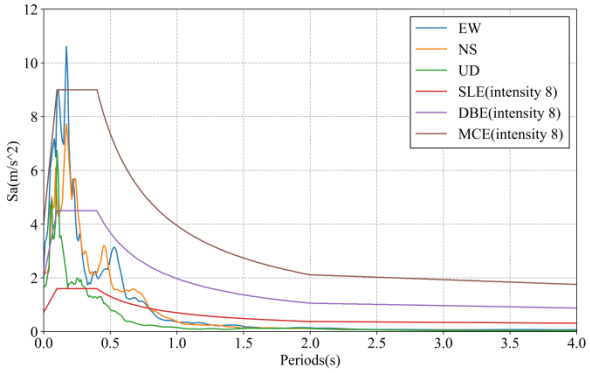

Figure 1 Response spectra of the recorded ground motions with maximal PGA

3. Damage analysis of the target region subjected to the recorded ground motions

Using the real-time ground motions obtained from the strong motion networks and the **city-scale nonlinear time-history analysis (see the Appendix of this report),** the damage ratios of buildings located in different places can be obtained. The building damage distribution and the human uncomfortableness distribution near to different stations is shown in Figure 2 and Figure 3, respectively. These outcomes can provide a reference for post-earthquake rescue work.

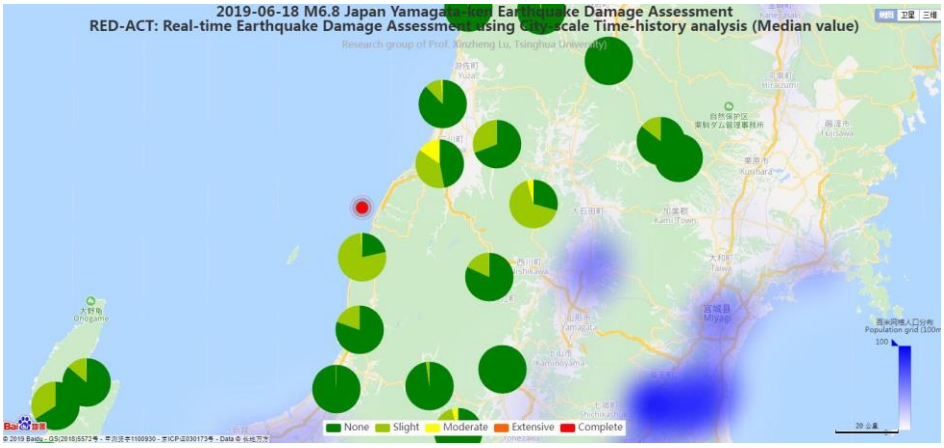

Figure 2 Damage ratio distribution of the buildings near to different stations

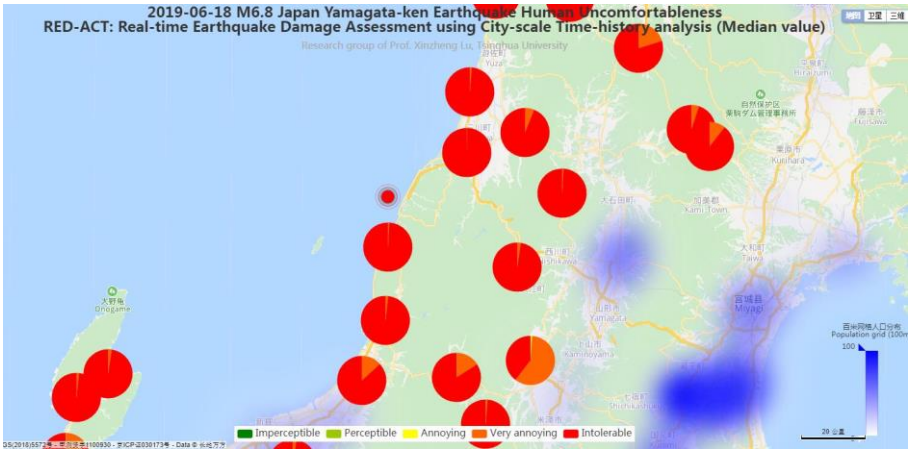

Figure 3 Human uncomfortableness distribution near to different stations

4. Earthquake-induced landslide of the target region subjected to the recorded ground motions

According to local topographic data, lithology data and ground motion records, the distribution of earthquake-induced landslide near to different stations under the different proportions of the landslide slab thickness that is saturated can be calculated, as shown in Figure 4. The basemap shows the distribution of the local slope. The number in the circle represents the critical slope of the landslide. The earthquake-induced landslide tends to occur with a higher probability when the slope near the station is larger than this threshold value.

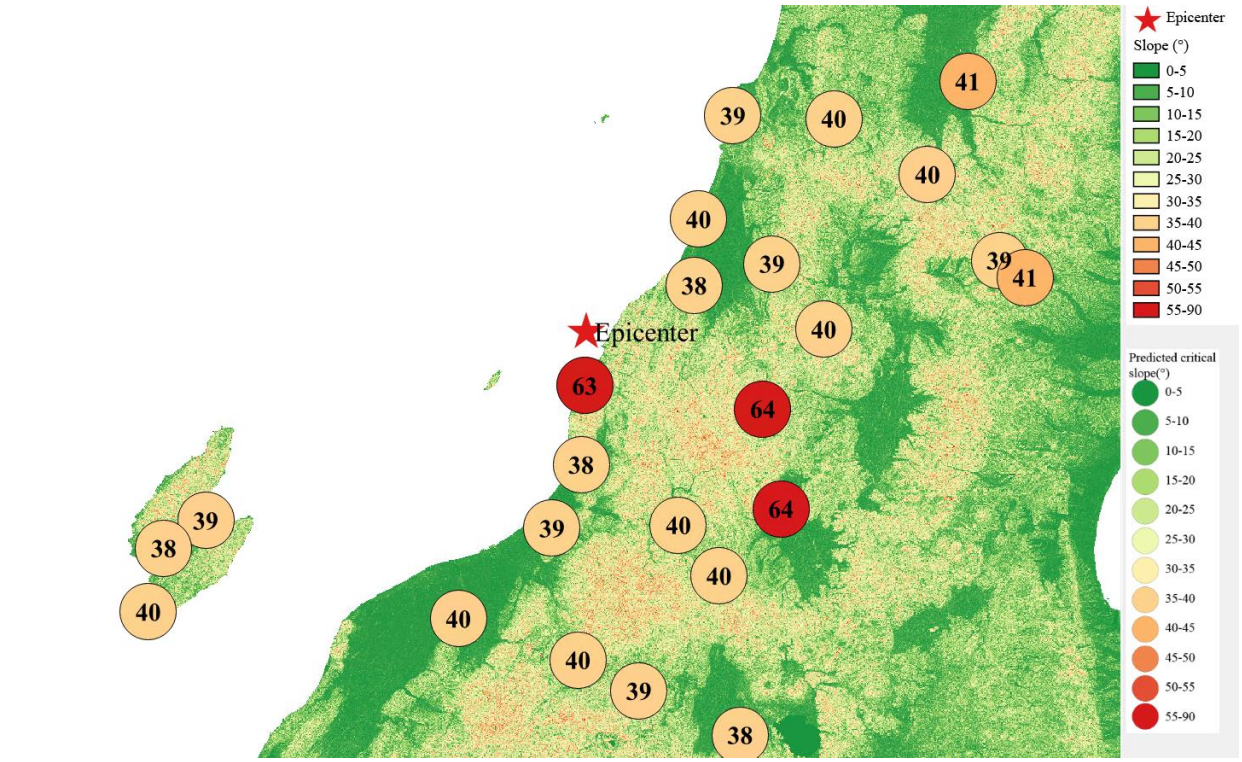

(a) The proportion of the landslide slab thickness that is saturated equals 0%

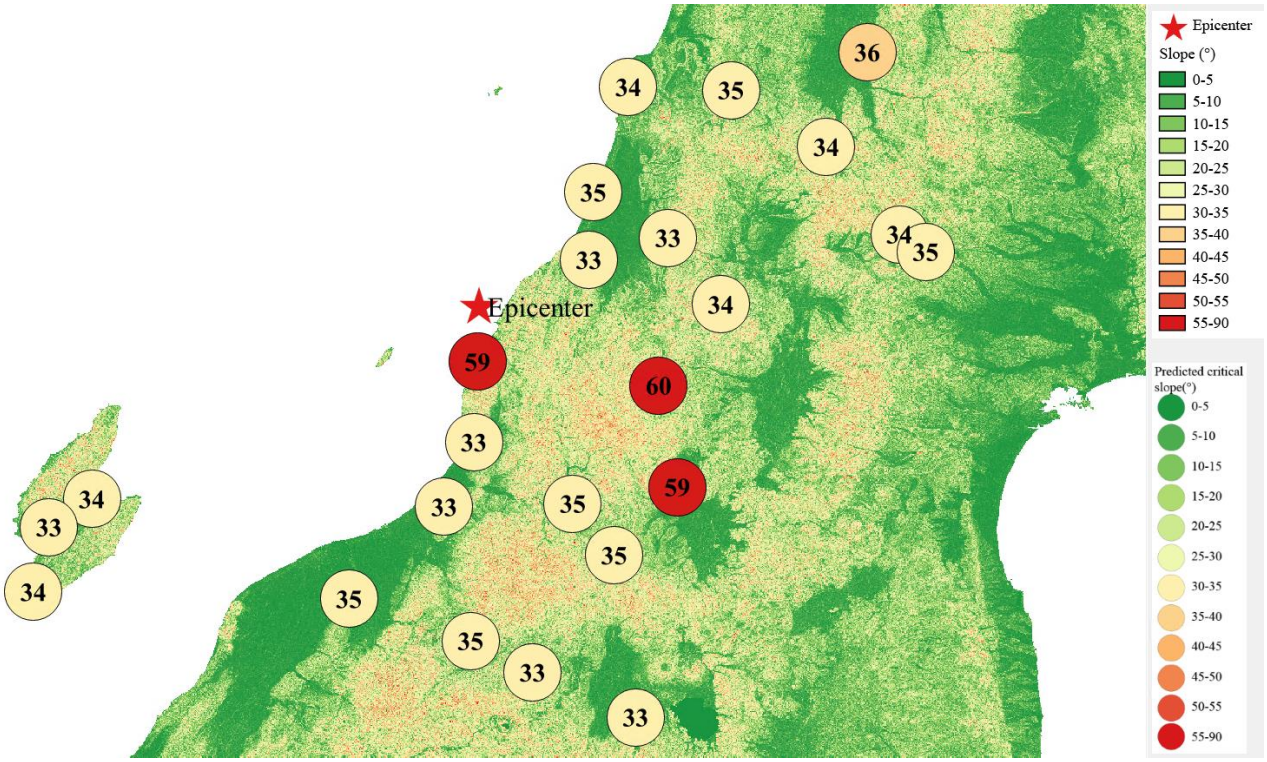

(b) The proportion of the landslide slab thickness that is saturated equals 50%

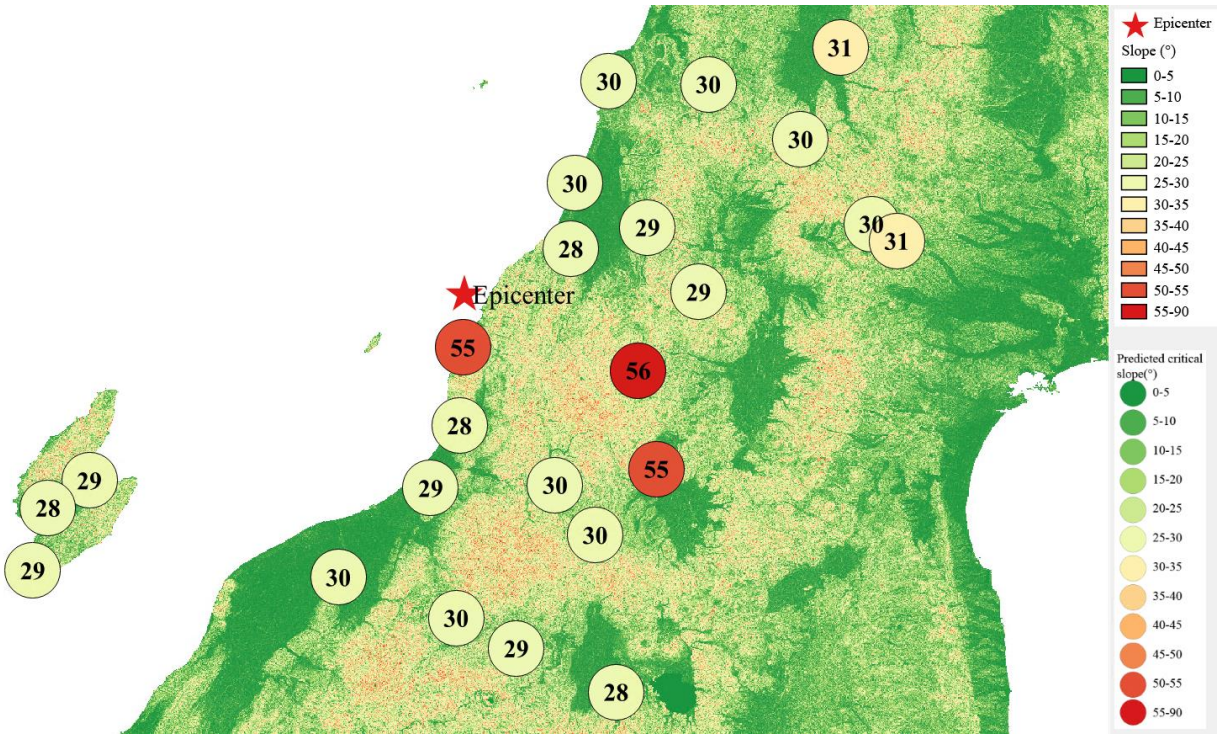

(c) The proportion of the landslide slab thickness that is saturated equals 90%

Figure 4 Distribution of earthquake-induced landslide near to different stations

Scientific background of this report can be found at: http://www.luxinzheng.net/software/Real-Time_Report.pdf

Table 1 Names and locations of the strong motion stations

No.	Station Name	Longitude	Latitude
1	AKT011	140.58	39.8128
2	AKT017	140.563	39.2975
3	AKT018	140.19	39.1939
4	AKT019	140.451	39.0384
5	AKT020	139.909	39.2022
6	FKS022	139.647	37.6002
7	FKS023	139.929	37.4774
8	MYG005	140.651	38.7992
9	MYG019	140.723	38.7513
10	NIG002	138.44	38.0745
11	NIG003	138.323	37.9976
12	NIG004	138.28	37.8205
13	NIG006	139.496	38.4501
14	NIG007	139.486	38.2301
15	NIG008	139.405	38.053
16	NIG011	139.144	37.8013
17	NIG012	139.477	37.6863
18	YMT001	139.813	38.914

19	YMT003	139.801	38.7292
20	YMT005	140.162	38.607
21	YMT008	139.992	38.3856
22	YMT012	140.043	38.1074
23	YMT013	139.757	38.0621
24	YMT014	139.87	37.9207
25	YMT016	140.018	38.7895